

AUTOMATION OF DNA COMPUTING READOUT METHOD BASED ON REAL-TIME POLYMERASE CHAIN REACTION IMPLEMENTED ON DNA ENGINE OPTICON 2 SYSTEM

M.F Mohamed Saaid¹, Z. Ibrahim¹, M. Khalid¹, S. Sudin², and N.H Sarmin³

¹Center for Artificial Intelligence and Robotics (CAIRO), Department of Mechatronics and Robotics

²Control & Instrumentation Engineering Department

Faculty of Electrical Engineering, Universiti Teknologi Malaysia, 81310 Skudai, Johor Darul Takzim, Malaysia

³Department of Mathematics, Fac. of Science, Universiti Teknologi Malaysia, 81310 Skudai, Johor, Malaysia

Email: ninjagaban@yahoo.com

ABSTRACT

In this paper, an automation of DNA computing readout method based on real-time Polymerase Chain Reaction (PCR) is developed, which employs a hybrid in vitro-in silico approach. In the in vitro phase, TaqMan-based real-time PCR reactions are performed in parallel, to investigate the ordering of pairs of nodes in the Hamiltonian Path Problem (HPP), in terms of relative distance from the DNA sequence encoding the known start node. The real-time PCR experiment is implemented on DNA Engine Opticon II system. Alternative Fuzzy C-Means (AFCM) clustering algorithm is used to identify automatically two different reactions in real-time PCR, followed by in silico algorithm, which in turn, enables extraction of the Hamiltonian path. A software called "SILICOIN" is built to implement the AFCM clustering and the in silico algorithm, which return the desired Hamiltonian path.

Keywords: DNA Computing, Fuzzy C-Means, real-time PCR, TaqMan probes.

INTRODUCTION

Since the discovery of the polymerase chain reaction (PCR) [1], numerous applications have been explored, primarily in the life sciences and medicine, and importantly, in DNA computing as well. The subsequent innovation of real-time PCR has rapidly gained popularity and plays a crucial role in molecular medicine and clinical diagnostics [2]. All real-time amplification instruments require a fluorescence reporter molecule for detection and quantitation, whose signal increase is proportional to the amount of amplified product.

A TaqMan DNA probe is a modified, nonextendable duallabeled oligonucleotides. The 5' and 3' ends of the oligonucleotide are terminated with an attached reporter, such as FAM, and quencher fluorophores dyes, such as TAMRA, respectively, as shown in Figure 1 [3]. Upon laser excitation at 488 nm, the FAM fluorophore, in isolation emits fluorescence at 518 nm. Given proximity of the TAMRA quencher, however, based on the principle of fluorescence resonance energy transfer (FRET), the excitation energy is not emitted by the FAM fluorophore, but rather is transferred to TAMRA via the dipole-dipole interaction between FAM and TAMRA. As TAMRA emits this absorbed energy at significantly wavelengths (580 nm), the resulting fluorescence is not observable in Channel 1 of real-time PCR instruments [4].

The combination of dual-labeled TaqMan DNA probes with forward and reverse primers is a must for a successful real-time PCR. As PCR is a repeated cycle of three steps (denaturation, annealing, and polymerization), a TaqMan DNA probe will anneal to a site within the DNA template in between the forward and reverse primers during the annealing step, if a subsequence of the DNA template is complementary to the sequence of the DNA probe. During polymerization, *Thermus aquaticus (Taq)* DNA polymerase will extend the primers in a 5' to 3' direction. At the same time, the *Taq* polymerase also acts as a "scissor" to degrade the probe via cleavage, thus separating the reporter from the quencher, as shown in Figure 2 [5], where R and Q denote the reporter dye and quencher dye, respectively. This separation subsequently allows the reporter to emit its fluorescence [6]. This process occurs in every PCR cycle and does not interfere with the exponential accumulation of PCR product. As a result of PCR, the amount of DNA template increases exponentially, which is accompanied by a proportionate increase in the overall fluorescence intensity emitted by the reporter group of the excised TaqMan probes. Hence, the intensity of the measured fluorescence at the end of each PCR

polymerization is correlated to the total amount of PCR product, which can then be detected, using a real-time PCR instrument for visualization.



Figure 1: Illustration of the structure of a TaqMan DNA probe. Here, R and Q denote the reporter and quencher fluorophores, respectively

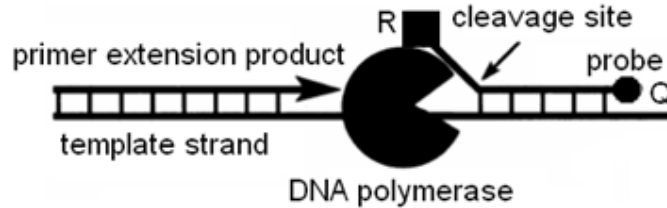


Figure 2: Degradation of a TaqMan probe, via cleavage by DNA polymerase

Previously, we proposed a readout method tailored specifically to the HPP in DNA computing, which employs a hybrid *in vitro-in silico* approach [7]. In the *in vitro* phase, $O(|V|^2)$ TaqMan-based real-time PCR reactions are performed in parallel, to investigate the ordering of pairs of nodes in the Hamiltonian path of a $|V|$ -node instance graph, in terms of relative distance from the DNA sequence encoding the known start node. The resulting relative orderings are then processed *in silico*, which efficiently returns the complete Hamiltonian path. The proposed approach is experimentally validated optical method specifically designed for the quick readout of HPP instances, in DNA computing. Previously, graduated PCR, which was originally demonstrated by Adleman [8], was employed to perform such operations. While a DNA chip based methodology, which makes use of biochip hybridization for the same purpose has been proposed [9-11], this method is more costly, and has yet to be experimentally implemented.

In this paper, an automation system for DNA computing readout method implemented on real-time PCR is developed, which consist of *in vitro-in silico* approach. The real-time amplification is performed with the TaqMan probes and the TaqMan detection mechanism was exploited for the design and development of the readout approach. The *in vitro* part is performed on the DNA Engine Opticon 2 System. As shown in Figure 3, the output of DNA computing readout method implemented on DNA Engine Opticon 2 System consist of two kinds of reactions, namely “YES” reaction and “NO” reaction. In the *in silico* information processing, Alternative Fuzzy C-Means (AFCM) [12] clustering algorithm is implemented for automatic classification of “YES” and “NO” reaction. A software called *SilicoIn* is developed and able to implement the *in silico* information processing during the *in silico* phase of readout approach in order to cluster the “YES” and “NO” reaction, followed by *in silico* algorithm which directly show the Hamiltonian path.

NOTATIONS AND BASIC PRINCIPLE

First of all, $v_{1(a)}v_{2(b)}v_{3(c)}v_{4(d)}$ denotes a double-stranded DNA (dsDNA) which contains the base-pair subsequences, v_1 , v_2 , v_3 , and v_4 , respectively. Here, the subscripts in parenthesis (a , b , c , and d) indicate the length of each respective base-pair subsequence. For instance, $v_{1(a)}$ indicates that the length of the double-stranded subsequence, v_1 is 20 base-pairs (bp). When convenient, a dsDNA may also be represented without indicating the segment lengths (e.g., $v_1v_2v_3v_4$).

A reaction denoted by $\text{TaqMan}(v_0, v_k, v_l)$ indicates that real-time PCR is performed using forward primer v_0 , reverse primer v_l , and TaqMan probe v_k . Based on the proposed approach, there are two possible reaction conditions regarding the relative locations of the TaqMan probe and reverse primer. In particular, the first condition occurs when the TaqMan probe specifically hybridizes to the template, between the forward and reverse primers, while the second occurs when the reverse primer hybridizes between the forward primer and the TaqMan probe. As shown in Figure 3, these two conditions would result in different amplification patterns during real-time PCR, given the same DNA template (i.e., assuming that they occurred separately, in two

different PCR reactions). The higher fluorescent output of the first condition is a typical amplification plot for real-time PCR. In contrast, the low fluorescent output of the second condition reflects the cleavage of a few of the TaqMan probes via DNA polymerase due to the ‘unfavourable’ hybridization position of the reverse primer. Thus, $TaqMan(v_0, v_k, v_l) = YES$ if an amplification plot similar to the first condition is observed, while $TaqMan(v_0, v_k, v_l) = NO$ if an amplification plot similar to the second condition is observed.

REAL-TIME PCR-BASED READOUT APPROACH

Let the output of an *in vitro* computation of an HPP instance of the input graph be represented by a 140-bp dsDNA $v_{0(20)}v_{1(20)}v_{4(20)}v_{2(20)}v_{5(20)}v_{3(20)}v_{6(20)}$, where the Hamiltonian path $V_0 \rightarrow V_1 \rightarrow V_4 \rightarrow V_2 \rightarrow V_5 \rightarrow V_3 \rightarrow V_6$, begins at node V_0 , ends at node V_6 , and contains intermediate nodes $V_1, V_4, V_2, V_5,$ and V_3 , respectively. Note that in practice, only the identities of the starting and ending nodes, and the presence of all intermediate nodes will be known in advance to characterize a solving path. The specific order of the intermediate nodes within such a path is unknown.

The first part of the approach, which is performed *in vitro*, consists of $[(|V|-2)^2-(|V|-2)]/2$ real-time PCR reactions, each denoted by $TaqMan(v_0, v_k, v_l)$ for all k and l , such that $0 < k < |V|-2, 1 < l < |V|-1$, and $k < l$. For this example instance, so that the DNA template is the dsDNA, $v_0v_1v_4v_2v_5v_3v_6$ these 10 reactions are as follows:

- (1) $TaqMan(v_0, v_1, v_2) = YES$
- (2) $TaqMan(v_0, v_1, v_3) = YES$
- (3) $TaqMan(v_0, v_1, v_4) = YES$
- (4) $TaqMan(v_0, v_1, v_5) = YES$
- (5) $TaqMan(v_0, v_2, v_3) = YES$
- (6) $TaqMan(v_0, v_2, v_4) = NO$
- (7) $TaqMan(v_0, v_2, v_5) = YES$
- (8) $TaqMan(v_0, v_3, v_4) = NO$
- (9) $TaqMan(v_0, v_3, v_5) = NO$
- (10) $TaqMan(v_0, v_4, v_5) = YES$

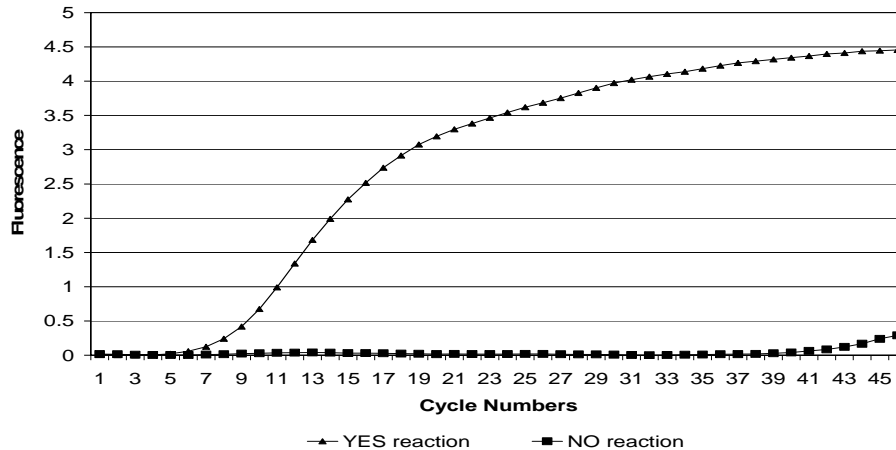


Figure 3: An example of reaction plots corresponding to $TaqMan(v_0, v_k, v_l) = YES$ (first condition) and $TaqMan(v_0, v_k, v_l) = NO$ (second condition)

Note that the overall process consists of a set of parallel real-time PCR reactions, and thus requires $O(I)$ laboratory steps for *in vitro* amplification. The accompanying SPACE complexity, in terms of the required number of tubes is $O(|V|^2)$. Clearly, only one forward primer is required for all real-time PCR reactions, while the number of reverse primers and TaqMan probes required with respect to the size of input graph are each $|V|-3$.

After all real-time PCR reactions are completed, the *in vitro* output is subjected to an algorithm for *in silico* information processing, producing the satisfying Hamiltonian path of the HPP instance in $O(n^2)$ TIME (here, n denotes vertex number).

The next step is to use all the information from the six TaqMan reactions to allocate each node of the Hamiltonian path. This can be done by applying the *in silico* algorithm, below.

```

Input: N[0...|V|-1]=2 // N[0, ?, ?, ?, ?, 6]
A[1...|V|-2]=|V| // A[1, 1, 1, 1, 1]
for k=1 to |V|-3
  for l=k+1 to |V|-2
    if TaqMan(v0,vk,vl) = YES
      A[l] = A[l]+1
    else A[k] = A[k]+1
    endif
  endfor
  N[ A[k] ] = k
endfor
N[ A[ |V|-2 ] ] = |V|-2

```

In this algorithm, an array (N[0...|V|-1]) that store all the nodes of the Hamiltonian path is defined. In addition, an array of aggregation values (A[1...|V|-2]) that is used to locate the Hamiltonian path in each array of nodes is also defined. Based on the modified algorithm, the input array N is first initialized to N={0,?,?,?,?,6} since the start and the end of the path are known, in advance. Next, the aggregation array A is initialized to A={1,1,1,1,1}. During the loop operations of the algorithm, the value of in the array A is increased in each iteration steps. The aggregation array A[i] is used for indexing the nodes array for each value of k. After the loop operation |V|-2 is assigned to the N[A[|V|-2]]. The output of the this *in silico* algorithm can be viewed by calling back all the nodes array N[0] to N[|V|-1]. The outcome of the this *in silico* algorithms is N={0,1,4,2,5,3,6}. Note that this algorithm can be done if all the information of TaqMan reactions is already achieved. This only can be done if clustering is applied to investigate “YES” and “NO” reaction.

EXPERIMENTS

Preparation of input molecules

A pool of 140-bp input molecules $v_{0(20)}v_{1(20)}v_{4(20)}v_{2(20)}v_{5(20)}v_{3(20)}v_{6(20)}$ is prepared, via standard protocol of parallel overlap assembly (POA) of singlestranded DNA strands (ssDNAs). For this purpose, 13 ssDNAs are required, including additional ssDNAs, which act as link sequences for self-assembly. These strands are listed in Table 1. After completion, amplification via PCR was performed using the same protocol as POA. The forward primers and reverse primers used for the PCR reaction were 5'-CGTCAAGGCCGTCTCTATAT-3' and 5'-GTAGATTAAGAAGGTGCGCG-3', respectively. The PCR product was subjected to gel electrophoresis and the resultant gel image was captured, as shown in Figure 4. The 140-bp band in lane 2 shows that the input molecules have been successfully generated. Afterwards, the DNA of interest is extracted. The final solution for real-time PCR was prepared via dilution of the extracted solution, by adding ddH₂O (Maxim Biotech, Japan) into 100 μ l.

Table 1: The required single-stranded dnas for the generation of input molecules

Name	DNA Sequences (5'-3')	Length
v ₀	CGTCAAGGCCGTCTCTATAT	20
v ₁	CCACTGGTTCTGCATGTAAC	20
v ₄	TCCACGCTGCACTGTAATAC	20
v ₂	TGGACAACCGCAGTTACTAC	20
v ₅	ATGCGCCAGCTTCTAACTAC	20
v ₃	AGGAAACCTCACGACAGTCT	20
v ₆	CGCGCACCTTCTTAATCTAC	20
v ₀ v ₁	GAACCAGTGGATATAGAGACGGCCTTGACG	30
v ₁ v ₄	GCAGCGTGGAGTTACATGCA	20
v ₄ v ₂	CGGTTGTCCAGTATTACAGT	20
v ₂ v ₅	GCTGGCGCATGTAGTAACTG	20
v ₅ v ₃	GAGGTTTCTGTAGTTAGAA	20
v ₃ v ₆	GTAGATTAAGAAGGTGCGCGAGACTGTCGT	30

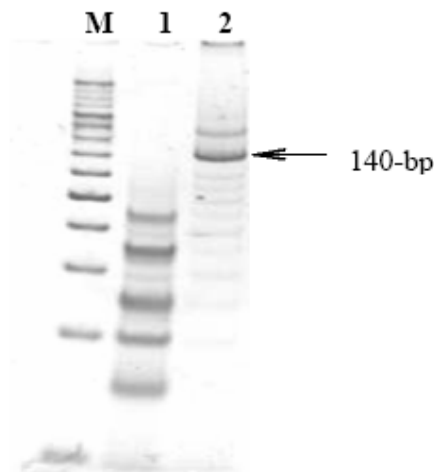


Figure 4: Gel image for the preparation of input molecules. Lane M denotes a 20-bp molecular marker, lane 1 is the product of initial pool generation based on parallel overlap assembly, and lane 2 is the amplified PCR product

Real-time PCR Experiments

The real-time PCR reaction involves primers (Sigma Genosys, Japan), TaqMan probes (Sigma Genosys, Japan), and QuantiTect Probe PCR Kit (QIAGEN, Japan). The sequences for forward primers, reverse primers, and TaqMan probes are listed in Tables 2 and Table 3. QuantiTect Probe PCR Kit essentially contains 3 vials of 2x Master Mix and 2 vials of RNase-free Water. The master mix contains HotStarTaq® DNA Polymerase, QuantiTect Probe PCR Buffer, dNTP mix including dUTP, ROX™ (passive reference dye), and 8 mM MgCl₂.

For real-time PCR, as recommended by the manufacturer, the final concentration of primers should be 0.4 μ M, whereas the final concentration of the DNA probes should be between 0.1-0.2 μ M. In this study, the maximum final concentration of probe, which is 0.2 μ M, was chosen and prepared. The real-time PCR was performed on a DNA Engine Opticon® 2 System (MJ Research, USA) where amplification is carried out in a 50 μ l tube. Each tube contains 25 μ l 2x PCR Master Mix, 0.4 μ l forward primer, 0.4 μ l reverse primer, 0.4 μ l probe, 2 μ l template, and 21.8 μ l RNase-free Ultrapure Water.

Ten separate real-time PCR reactions were performed in parallel, in order to implement the first stage of the proposed HPP readout. After the initial activation step at 95°C for 15 minutes, the amplification consists of 45 cycles of denaturation and annealing/extension, performed at 94°C for 15 s and 60°C for 60 s, respectively. The resulting real-time PCR amplification plots are illustrated in Figure 5.

Table 2: Sequences for forward primer and reverse primers employed for the real-time PCR

Primer	DNA Sequences (5'-3')	GC%	T_m (°C)
Forward primer, v_0	CGTCAAGGCCGCTCTATAT	0.5	59.1
Reverse primer, \bar{v}_4	GTATTACAGTGCAGCGTGGA	0.5	59.7
Reverse primer, \bar{v}_2	GTAGTAACTGCGGTTGTCCA	0.5	58.6
Reverse primer, \bar{v}_5	GTAGTTAGAAGCTGGCGCAT	0.5	59.5
Reverse primer, \bar{v}_3	AGACTGTCGTGAGGTTTCCT	0.5	58.7

Table 3: Sequences for TaqMan dual-labeled probes

TaqMan Probes	Sequences
Probe v_1	R – CCACTGGTTCATGTAAC – Q
Probe v_2	R – TGGACAACCGCAGTTACTAC – Q
Probe v_3	R – AGGAAACCTCACGACAGTCT – Q
Probe v_4	R – TCCACGCTGCACTGTAATAC – Q

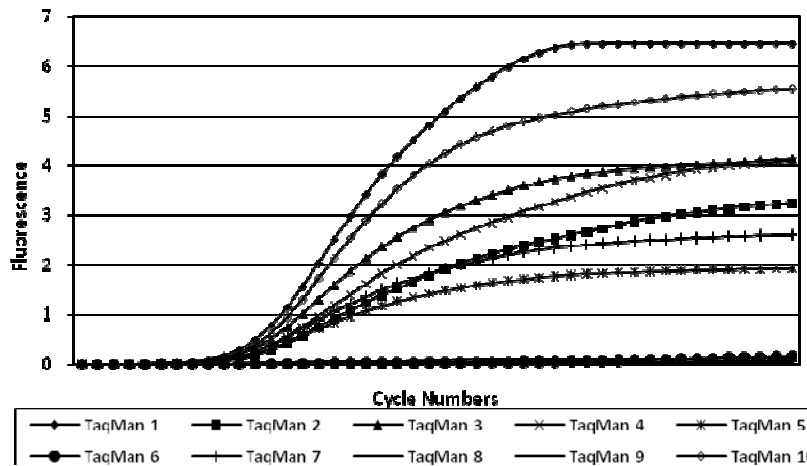


Figure 5: Output of real-time PCR. Reactions 1 to 10 indicate the $\frac{(|V|-2)^2 - (|V|-2)}{2}$ TaqMan(v_0, v_k, v_l) reactions of the input instance, as defined in Section 3. Note that reactions 6, 8, and 9, which correspond to “NO”, show virtually no amplification

IN SILICO INFORMATION PROCESSING

Exporting data

The data from DNA Engine Opticon 2 System can be exported by clicking the export data on the software. From the data, only the FAM reading was selected to be exported into the SilicoIn software, since the FAM emission reading is the actual result of TaqMan reaction shown in Figure 5. The exporting process was done after the in vitro phase is already completed. This exported data were written in the text file format, which show the fluorescence intensity from the first to the 46th thermal cycle for all 10 different TaqMan reactions.

Clustering algorithm

From the output graph of real-time PCR, an unsupervised learning such as clustering algorithm can be implemented for automatic classification of a data [13]. Clustering algorithm, K-means for example is easy to implement, since the number of groups for classification of TaqMan reactions are already known. However, hard partitioning or non-fuzzy clustering algorithm requires an exhaustive search in a huge space because some variables can only take two values 0 and 1. Meanwhile fuzzy clustering is more computational tractability than hard partitioning algorithm [14]. Hence, all the variables are continuous, so that derivatives can be computed to find the right direction for the search [15].

Fuzzy C-means (FCM) has become the well known and powerful method in cluster analysis, and has been applied in many fields. However FCM clustering algorithm cannot handles noise and outliers data. Thus, AFCM clustering algorithm has been developed by Wu and Yang, to enhance the robustness of FCM to noise and outliers as well as tolerate with unequal sized clusters [12].

FCM is a data clustering technique, which is based on the optimization of the objective function [16]:

$$J(U, Y) = \sum_{i=1}^C \sum_{j=1}^N (\mu_{ij})^m \|x_j - y_i\|^2 \tag{1}$$

where C is a number of clusters and N is a number of data. Every data point in the data set requires to belong to a cluster at a particular membership degree. The purpose of FCM is to group data points into different specific clusters. Let $X = \{x_1, x_2, \dots, x_N\}$ be a collection of data. By minimizing (1), X is classified into C homogeneous clusters, where μ_{ij} is the membership degree of data x_j to a fuzzy cluster set y_i , $Y = \{y_1, y_2, \dots, y_C\}$ are the cluster

centers. $U=(\mu_{ij})_{N \times C}$ is a fuzzy partition matrix, and μ_{ij} indicates the membership degree of each data point in the data set to the cluster i . The value of U should satisfy the following conditions:

$$\mu_{ij} \in [0,1], \quad \forall i = 1, \dots, C, \forall j = 1 \dots N \tag{2}$$

$$\sum_{i=1}^C \mu_{ij} = 1, \quad \forall j = 1, \dots, N \tag{3}$$

The $\|x_j - y_i\|$ is the Euclidean distance between x_j and y_i . The parameter m is called fuzziness value index, which control the fuzziness value of membership of each datum. The cluster center can be calculated by using the following equation

$$y_i = \frac{\sum_{j=1}^N (\mu_{ij})^m x_j}{\sum_{j=1}^N (\mu_{ij})^m}, \quad \forall i = 1, \dots, C \tag{4}$$

Then, clustering can be achieved by iteratively minimize the aggregate distance between each data point in the data set and cluster centers until no further minimization is possible. Then, the fuzzy partition matrix U is updated by using following equation

$$\mu_{ij} = \frac{1}{\sum_{k=1}^C \left(\frac{\|x_j - y_i\|}{\|x_j - y_k\|} \right)^{\frac{2}{m-1}}} \tag{5}$$

Wu and Yang have shown that Euclidean norm is not robust in a noisy environment [12]. Thus, they proposed the exponential distance metric to replace the Euclidean distance in the objective function. The exponential distance is given by

$$d(x_j, y_i) = \left(1 - \exp\left(-\beta \|x_j - y_i\|^2\right) \right)^{1/2} \tag{6}$$

where β is a positive constant, defined by

$$\beta = \left(\frac{\sum_{j=1}^N \|x_j - \bar{x}\|^2}{N} \right)^{-1} \tag{7}$$

and \bar{x} is defined as

$$\bar{x} = \left(\frac{\sum_{j=1}^N x_j}{N} \right) \tag{8}$$

By replacing Euclidean distance with the exponential distance, the new objective function is formulated as

$$J(U, Y) = \sum_{i=1}^C \sum_{j=1}^N (\mu_{ij})^m \left(1 - \exp(-\beta \|x_j - y_i\|^2) \right) \quad (9)$$

which defines the formulation of AFCM clustering algorithm. The necessary condition for minimizing equation (9) is given in equation (10) and (11)

$$\mu_{ij} = \frac{1}{\sum_{k=1}^C \left(\frac{(1 - \exp(-\beta \|x_j - y_i\|^2))}{(1 - \exp(-\beta \|x_j - y_k\|^2))} \right)^{\frac{1}{m-1}}} \quad (10)$$

$$y_i = \frac{\sum_{j=1}^N (\mu_{ij})^m \exp(-\beta \|x_j - y_i\|^2) x_j}{\sum_{j=1}^N (\mu_{ij})^m \exp(-\beta \|x_j - y_i\|^2)} \quad (11)$$

A fixed-point iteration method can be implemented for calculating the y_i .

In order to cluster the results of TaqMan reaction, namely “YES” and “NO” reaction, each graph of the reactions are represented as vector $\mathbf{x}_j = \{x_{j(1)}, x_{j(2)}, x_{j(3)}, \dots, x_{j(45)}, x_{j(46)}\}$. The reactions are clustered into two groups, having their centre at $\mathbf{y}_1 = \{y_{1(1)}, y_{1(2)}, \dots, y_{1(45)}, y_{1(46)}\}$ and $\mathbf{y}_2 = \{y_{2(1)}, y_{2(2)}, \dots, y_{2(45)}, y_{2(46)}\}$. The two centres can be viewed as graphs that similar to the TaqMan reaction “YES” and “NO”. It is noticed that the centre that is located in the amplification region always have greater value than the other center in the non-amplification region. The two centers are called as “YES” and “NO” center, where “YES” center is greater than “NO” center. This information is used to classify the TaqMan reactions “YES” and “NO” by comparing the fuzzy partition matrix U . If \mathbf{y}_2 represents the “YES” center and \mathbf{y}_1 represent the “NO” center (note that \mathbf{y}_2 is not always represent the “YES” center when the FCM algorithm is implemented), then $\mathbf{y}_2 > \mathbf{y}_1$. For example, if μ_{11} and μ_{12} equals to 0.6 and 0.4, respectively, the “YES” and “NO” reaction can be determined by following this rule

if ($\mathbf{y}_1 > \mathbf{y}_2$ and $\mu_{i1} > \mu_{i2}$) or ($\mathbf{y}_2 > \mathbf{y}_1$ and $\mu_{i2} > \mu_{i1}$)
 $\mathbf{x}_j =$ “YES”
 else $\mathbf{x}_j =$ “NO”

Based on the proposed rule, \mathbf{x}_j is classified as “NO” reaction since $\mu_{i1} > \mu_{i2}$ and $\mathbf{y}_1 < \mathbf{y}_2$. This rule is applied to the remaining “YES” and “NO” reactions. The whole classification process for FCM and AFCM can be described in the following steps

FCM

Step 1: Initialize the membership matrix U with random values, subject to (2) and (3)

Step 2: Calculate the cluster center Y by using (4)

Step 3: Update fuzzy partition matrix U by using (5)

Step 4: Stop if $\|U(t+1) - U(t)\| < e$, otherwise go to step 2

Step 5: Determine “YES” and “NO” centers (either $\mathbf{y}_1 > \mathbf{y}_2$ or $\mathbf{y}_2 > \mathbf{y}_1$)

Step 6: Classify each TaqMan reactions by using the predefined rule

AFCM

Step 1: Initialize the membership matrix U with random values, subjected to conditions (2) and (3)

Step 2: Calculate the cluster center Y by solving the equation (11), and calculate for each dimension of Y .

Step 3: Update fuzzy partition matrix U based on (10)

Step 4: Stop if $\|U(t+1) - U(t)\| < e$, otherwise go to step 2

Step 5: Determine “YES” and “NO” centers (either $\mathbf{y}_1 > \mathbf{y}_2$ or $\mathbf{y}_2 > \mathbf{y}_1$)

Step 6: Classify each TaqMan reactions by using the predefined rule

RESULTS AND DISCUSSION

As discussed previously, in the *in vitro* phase of the readout approach, each real-time PCR reaction is mapped to a binary output (i.e., either “YES” or “NO”), based on the occurrence or absence of an exponential amplification. Given the existence of this mapping, the subsequent *in silico* information processing is capable of determining the Hamiltonian path of the input instance (e.g., $V_0 \rightarrow V_1 \rightarrow V_4 \rightarrow V_2 \rightarrow V_5 \rightarrow V_3 \rightarrow V_6$, for the example instance).

The amplification responses observed in this study differ from the amplification responses which are typically obtained in the life sciences and medicine. In particular, while in life science and medical applications, the initial copy number of the DNA template is normally very low, in the current study the input molecule is actually a DNA species extracted from a polyacrylamide gel, which exists at a high concentration. That is the main reason why the amplification signals in the current study appeared more rapidly than normal.

FCM and AFCM are implemented to classify the TaqMan reaction produced by the DNA Engine Opticon 2. The clustering parameters used are $e=0.00001$, $m=2$, $N=10$, and $C=2$. The algorithms are validated first on Matlab 7.0. The results are shown in Figure 6, and Figure 7. The fuzzy partition membership values for those two different algorithms are listed in Table 4. Based on Table 1, two misclassifications occurred when the conventional FCM is applied. On the other hand, the AFCM has correctly classified all the TaqMan reactions. Based on the amplification output of TaqMan reactions, reactions 1 and 10 are clearly out of range from the “YES” group, reactions 6, 8 and 9 are closely grouped together to form “NO” group, and reactions 2,3,4,5 and 7 can be viewed as “YES” group. The misclassification, occurred for the FCM, is affected by reactions 1 and 10, as the FCM clustering algorithm is based on the “means” or “average”. From this observation, reactions 1 and 10 can be classified as outliers or noises.

The misclassification problem can be corrected by using different distance measure such as exponential Euclidean distance, which is employed by AFCM. Table 1 shows that the AFCM has correctly classified all the TaqMan reaction, which proves that the exponential distance is more robust than Euclidean distance, in terms of handling of outliers and noises.

The “SILICOIN” software were built based on Visual C++ 6.0 running on Microsoft window xp. Tthis software is able to analyzed only 7 nodes of HPP problem. As shown in Figure 8, the exported data can be plot back in this software to visualize the difference between the “YES” and “NO” reaction. This software is able to cluster the TaqMan reactions, by implementing the AFCM algorithm based on the results shown by using Matlab 7.0. The *in silico* algorithm to obtain the Hamiltonian Path is also implemented in this software.

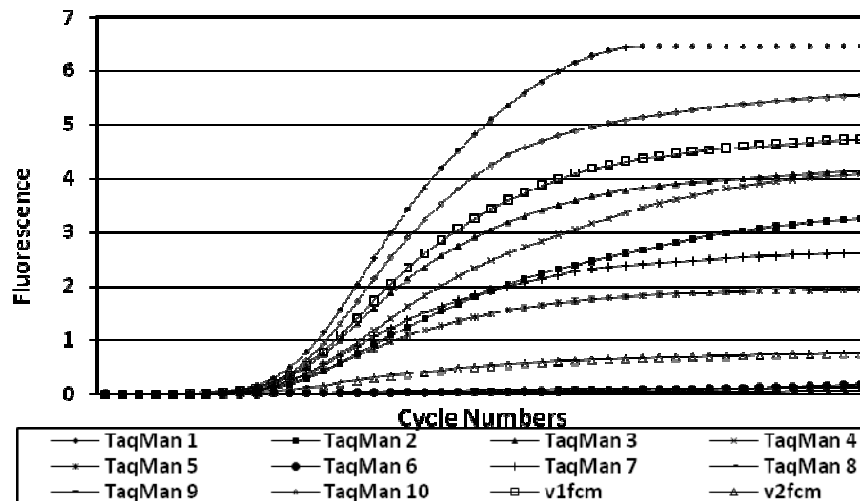


Figure 6: Output of real-time PCR. with “YES” and “NO” centers calculated using FCM clustering algorithm

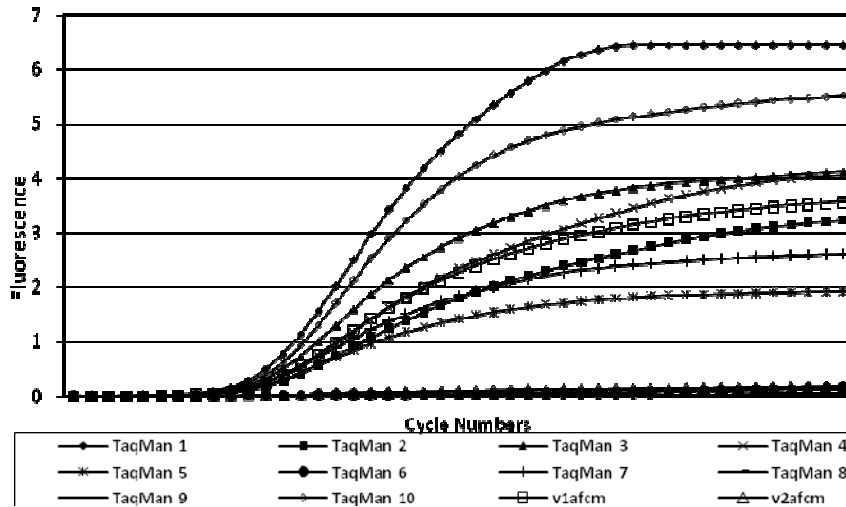


Figure 7: Output of real-time PCR. with “YES” and “NO” centers calculated using AFCM clustering algorithm

Table 4: Fuzzy partition value for each TaqMan reactions

TaqMan	manual	FCM		Reaction ($y_1 > y_2$)	AFCM		Reaction ($y_1 > y_2$)
		μ_{i1}	μ_{i2}		μ_{i1}	μ_{i2}	
1	YES	0.89454	0.10546	YES	0.52675	0.47325	YES
2	YES	0.60642	0.39358	YES	0.93949	0.060506	YES
3	YES	0.97209	0.027907	YES	0.90602	0.093975	YES
4	YES	0.90606	0.093941	YES	0.97078	0.029225	YES
5	YES	0.17222	0.82778	NO	0.58404	0.41596	YES
6	NO	0.018769	0.98123	NO	0.000716	0.99928	NO
7	YES	0.45078	0.54922	NO	0.8486	0.1514	YES
8	NO	0.021623	0.97838	NO	0.00265	0.99735	NO
9	NO	0.017352	0.98265	NO	0.000141	0.99986	NO
10	YES	0.96744	0.032556	YES	0.61813	0.38187	YES

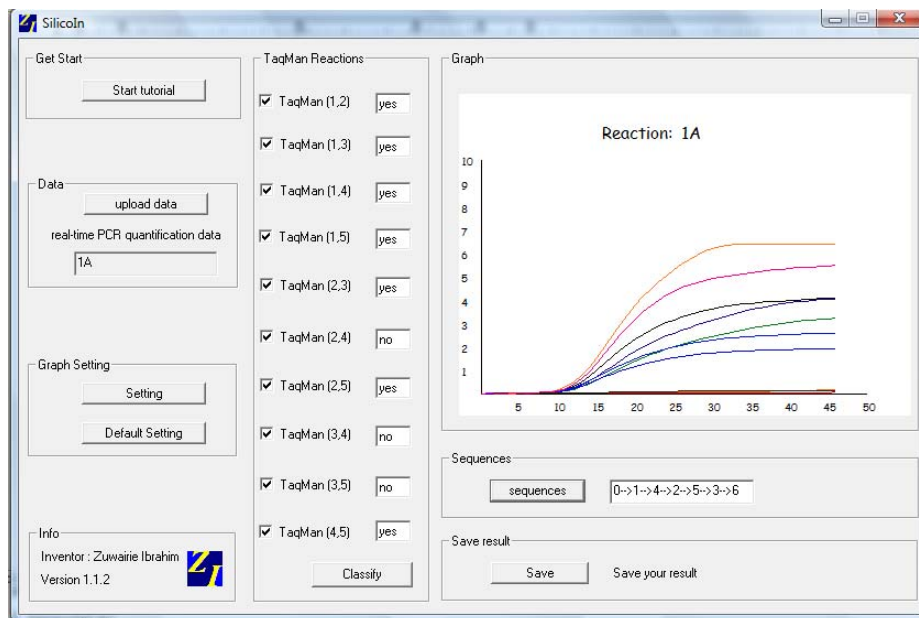


Figure 8: The clustering process and the Hamiltonian Path computed in “SILICOIN”

CONCLUSIONS

This research offers an automation of real-time PCR-based readout approach for DNA computing, which is implemented on DNA Engine Opticon 2 System. According to the experimental results, the amplification response for “YES” and “NO” reactions can be clearly distinguished. The *in silico* information of the real-time PCR readout method is computerized in the “SILICOIN” to cluster the TaqMan reaction the Hamiltonian Path automatically. By applying the AFCM clustering algorithm on the output results of real-time PCR, two different TaqMan reactions, “YES” and “NO”, can be clearly distinguished. Other algorithms that can handle noises and outliers can also be implemented to automatically classify the output of real-time PCR. Implementation of AFCM can also be discussed further so that the implementation can be fully maximized.

ACKNOWLEDGEMENT

This research is supported financially by the Ministry of Higher Education (MOHE) under Fundamental Research Grant Scheme (FRGS) (Vot 78225) and partly supported by the Ministry of Science, Technology, and Innovation (MOSTI) under eScienceFund (Vot 79027). Muhammad Faiz Mohamed Saaid is indebted to Universiti Teknologi Malaysia for granting him a financial support and opportunity to do this research.

REFERENCES

- [1] Mullis, K. (1986) Specific enzymatic amplification of DNA in vitro: the polymerase chain reaction, Cold Spring Harbor Symposium on Quantitative Biology.
- [2] Overbergh, L. (2003) The use of real-time reverse transcriptase PCR for the quantification of cytokine gene expression, *Journal of Biomolecular Techniques*.
- [3] Walker, N.J. (2002) A technique whose time has come, *Science*.
- [4] Lakowicz, J.R. (1999) *Principles of fluorescence spectroscopy*, 2nd Ed., Kluwer Academic/Plenum Publishers, New York.
- [5] Heid, C.A. (1996) Real-time quantitative PCR. *Genome Research*.
- [6] Holland, P.M. (1991) Detection of specific polymerase chain reaction product by utilizing the 5’_3’ exonuclease activity of *termus aquaticus* DNA polymerase, *Proceedings of the National Academy of Sciences of the United States of America*.
- [7] Ibrahim, Z., Rose, J. A., Suyama, A. and Khalid, M. (2008) Experimental Implementation and Analysis of a DNA Computing Readout Method Based on Real-Time PCR with TaqMan Probes, *Natural Computing Journal*, Springer.
- [8] Adleman, L. (1994) Molecular Computation of Solutions to Combinatorial Problems, *Science*.
- [9] Rose, J.A. (1997) The Effect of Uniform Melting Temperatures on the Efficiency of DNA Computing, DIMACS Workshop on DNA Based Computers III.
- [10] Wood, D.H. (1998) A DNA computing algorithm for directed Hamiltonian paths, *Proceedings of the Third Annual Conference on Genetic Programming*.
- [11] Wood, D.H., Clelland, C.L.T. and Bancroft, C. (1999) Universal biochip readout of directed Hamiltonian path problems, *Lecture Notes in Computer Science*, (pp.168-181). Springer
- [12] Wu, K.L. and Yang M.S. (2000) Alternative C-Means Clustering Algorithm, *Pattern Recognition*.
- [13] Everitt, B., Landau, S. and Leese, M. (2001) *Cluster Analysis*. London: Arnold.
- [14] Bezdek, J.C. (1974) Cluster Validity with Fuzzy Sets, *J. Cybernetics*.

- [15] Wang, L.X. (1997) *A Course of Fuzzy Systems and Control*. Prentice Hall.
- [16] Bezdek, J. (1981) *Pattern Recognition with Fuzzy Objective Function Algorithms*, Plenum Press, New York.

NOMENCLATURE

v_i	double-stranded DNA
V_i	Hamiltonian path nodes
U	fuzzy partition matrix
Y	set of cluster centre
X	set of data
x_j	data
μ_{ij}	membership value
y_i	cluster centre
$GC\%$	GC percentage
T_m	melting temperature